Papers

Variability of coastal water hydrodynamics in the southern Baltic – hindcast modelling of an upwelling event along the Polish coast

ANDRZEJ JANKOWSKI
Institute of Oceanology,
Polish Academy of Sciences,
Powstańców Warszawy 55, PL–81–712 Sopot, Poland;
e-mail: jankowsk@iopan.gda.pl

Abstract

This paper presents the results of an attempt to reproduce, with the aid of a numerical circulation model, the hydrological conditions observed in the coastal area of the southern Baltic in September 1989. A large fall in surface layer seawater temperature was recorded in September 1989 at two coastal stations in the vicinity of Kołobrzeg and Władysławowo. This upwelling-like phenomenon was assumed to be related to the specific anemobaric situation in September 1989, however typical of this phenomenon to occur along the Polish Baltic coast (Malicki & Miętus 1994). A three-dimensional (3-D) σ-coordinate baroclinic model of the Baltic Sea, with a horizontal resolution of $\sim$5 km and 24 sigma-levels in the vertical, was applied to investigate water circulation and thermohaline variability. Hindcast numerical simulation showed that the model provided a good reproduction of the temporal history of the surface seawater temperature and the duration of the upwelling-like fall, but that the model results were underestimated. The maxima of this large fall in the surface layer temperature at both coastal stations are closely related to the phase of change of the upwelling-favourable wind direction to the opposite one. The results of simulation runs showed details of upwelling development due to wind field fluctuations in time and differences in shaping the temperature and current patterns in conjunction with the variations in topography and coastline features in some areas along the Polish coast. Two different hydrodynamic regimes of water movements along the coast resulting from topographical features (the Słupsk Bank)

can be distinguished. From the model simulation the specific conditions for the occurrence and development of upwelling at the eastern end of the Polish coast (in the vicinity of Władysławowo) can be deduced.

1. Introduction

Upwelling occurs when cold water from the lower layers of the oceans is raised towards the surface. Wind-induced upwelling of cold water is a phenomenon often observed on the coasts of oceans, shelf seas and large inland waters (see e.g. Csanady 1982, Robinson 1985). It is generally assumed that Ekman offshore transport in the surface layer, generated by a longshore wind blowing with the coast to the left (in the northern hemisphere), is compensated by the upwelling of cold water. A physical and theoretical description of upwelling can be found in e.g. Smith (1968), Gill & Clarke (1974), Gill (1982).

The large-scale wind-induced (Ekman) upwelling is well known, for example, from off the west coasts of North and South America in the Pacific Ocean and off West and South Africa in the Atlantic on an oceanic scale (Robinson 1985). On a smaller scale, wind-induced upwelling also occurs in semi-enclosed shelf seas like the Baltic (Gidhagen 1984, Hansen et al. 1993, Meier 1999).

Infrared satellite images provide compelling evidence for upwelling along the Baltic coast. Svansson (1975), Gidhagen (1984), Bychkova & Victorov (1987), Bychkova et al. (1988), Hansen et al. (1993), Siegel et al. (1994), Urbański (1995), and Kręzel (1997) have shown by their analyses of satellite images that upwelling is a frequent occurrence in the Baltic Sea. The upwelling of cold coastal water during summer is a common event along the Polish and Swedish Baltic coasts (Gidhagen 1984, Bychkova & Victorov 1987, Bychkova et al. 1988, Urbański 1995, Kręzel 1997).

There have been some *in situ* measurements and observations (Svansson 1975, Fennel & Sturm 1992, Haapala 1994, Fennel & Seifert 1995, Schmidt et al. 1998, Matciak et al. 2001), of upwelling events occurring in different regions of the Baltic Sea. However, they are not complete enough to allow reconstruction of the coastal circulation.

Only a few attempts have been made to investigate coastal upwelling phenomena in different regions of the Baltic Sea with 3-D numerical models (see e.g. Fennel & Seifert 1995, Kowalewski 1998, Jankowski 2000). In the latter two studies, in which upwelling was investigated under homogeneous wind conditions over a model sea area, it was pointed out that E and SE winds favour upwelling water movements along the Polish Baltic coast.

In order to investigate many environmental problems in the coastal areas of the Baltic Sea it is necessary to know the time-dependent three-dimensional temperature distribution and circulation patterns which are frequently dominated by wind-induced upwelling. Upwelling can be assumed to be an effective mechanism leading to better mixing between the denser deep water and the less dense surface water in the Baltic as a whole. Therefore, a better understanding of this process will provide better predictions for this environment.

An intriguing case of upwelling along the Polish Baltic coast was reported by Malicki & Miętus (1994). The surface seawater temperatures recorded in September 1989 at two coastal stations (off Kołobrzeg and Władysławowo) on the Polish coast exhibited a large upwelling-like fall (variations of the order of 10 units (°C)) and a duration of several days (Fig. 1). This hydrological event was assumed to be related to the
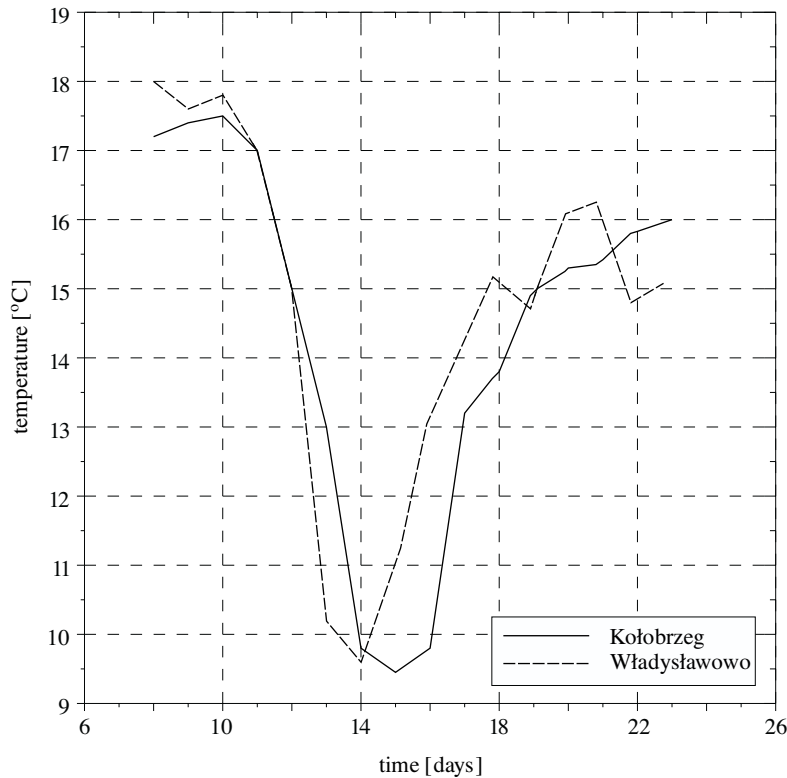

Fig. 1. Temporal history of the observed sea surface layer temperature [°C] in September 1989 at the Kołobrzeg and the Władysławowo stations on the Polish coast of the Baltic Sea elaborated from data taken from a figure in Malicki & Miętus (1994). Location of the stations and points – see Fig. 3
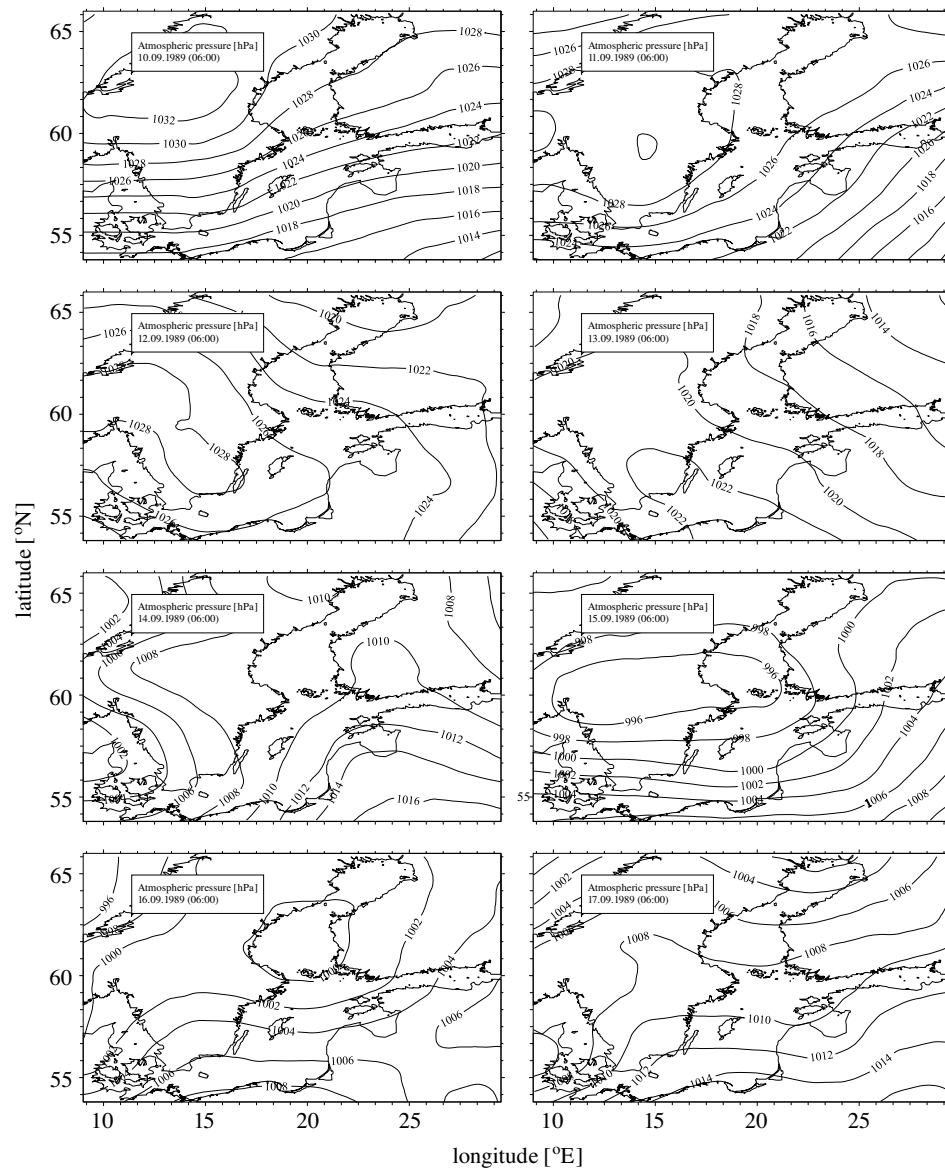
Fig. 2. Anemobaric situation above the Baltic Sea related to the abrupt fall in temperature along the Polish Baltic coast in September 1989 (from 10.09.89 to 17.09.89). Data taken from BED (2000). Isobars in [hPa]

anemobaric situation obtaining in September 1989, reproduced in Fig. 2 on the basis of meteorological data from BED (2000). Malicki & Miętus (1994) classified this anemobaric situation as typically causing a large fall in seawater surface temperature along the Polish Baltic coast.

The satellite data discussed by Krężel (1997) revealed the upwelling regions along the Polish coast (the western part, off Kołobrzeg, southwest of Kołobrzeg and off the open-sea coast of the Hel Peninsula) on 13 September 1989. In the area off the Hel Peninsula, upwelling events probably occur each year, often in September[1].

The main aim of this study is to reconstruct, with the aid of a numerical model, the hydrological conditions observed in the coastal area of the southern Baltic in September 1989.

The objective of this paper is to describe and make a preliminary analysis of the dynamic processes related to this upwelling-like event, a large fall in seawater surface temperature along the Polish coast of the southern Baltic.

The 3-D (σ-coordinate) model has been used here for hindcast simulations. The model is based on the Princeton Ocean Model code of Blumberg & Mellor (1987) and Mellor (1993), known as POM, and was adapted to Baltic Sea conditions (Jankowski 2000, 2002).

It is believed that the results of numerical simulations have supplied a new insight into the dynamics of the upwelling induced by real atmospheric forcing along the Polish Baltic coast.

The paper is arranged as follows. Section 2 presents basic information on model equations and boundary conditions. Then, in Section 3, some details of the calculations of initial fields and atmospheric forcings are outlined. Section 4 gives the results of the numerical experiments and simulations, together with a discussion of the model results. Finally, some conclusions are given in Section 5.

2. Model description

The model domain comprises the entire Baltic with its main basins: the Gulf of Bothnia, the Gulf of Finland, the Gulf of Riga, the Belt Sea, Kattegat and Skagerrak. At the open boundary in the Skagerrak simplified, radiation type, boundary conditions were applied. The bottom topography of the Baltic Sea used in the model is based on data from Seifert & Kayser (1995) (Fig. 3). With a horizontal resolution of $\sim$5 km and with 24 σ-levels in the vertical, the model allows variability as well as mesoscale features of the order of 10 km of the currents and thermohaline fields in the Baltic to be investigated and reproduced.

---

[1]Dr Krężel, from the Institute of Oceanography of the University of Gdańsk, documented the occurrence of upwelling in the vicinity of the Hel Peninsula based on satellite sea surface mapping during the Seminar of Polish SCOR on 26 October 2000, Gdynia: 'Upwelling in the Baltic Sea: its occurrence, present state of knowledge, research methods, modelling prospects', (in Polish).
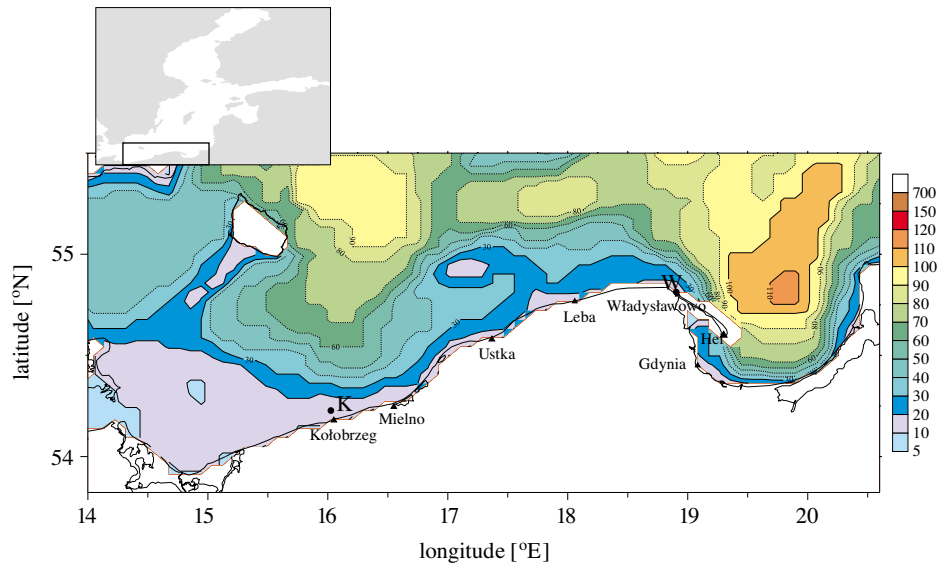
Fig. 3. The study area, the location of the Kołobrzeg and Władysławowo stations and the location of points used for visualizing the temporal evolution of the calculated hydrological parameters. The bottom topography was elaborated on the basis of data from Seifert & Kayser (1995). Isobaths in metres

Only a limited description of the model will be provided here to help the reader appreciate the simulation results. For further details of the POM model the reader is referred to Blumberg & Mellor (1987) and Mellor (1993), and for details of the Baltic version to Jankowski (2000, 2002).

2.1. Equations and boundary conditions

The model (Blumberg & Mellor 1987, Mellor 1993, Jankowski 2002 – hereafter referred to as AJ) solves the finite-difference analogue of the following set of equations assuming that the sea is an incompressible and hydrostatic fluid, and using the Boussinesq approximation:

$$\partial \boldsymbol{u}/\partial t + \boldsymbol{u} \cdot \nabla \boldsymbol{u} + w \partial \boldsymbol{u}/\partial z + f \boldsymbol{k} \times \boldsymbol{u} =$$

$$= -\frac{1}{\rho_0} \nabla p + \partial (A_v \partial \boldsymbol{u}/\partial z)/\partial z + \boldsymbol{F}_u, \tag{1}$$

$$\partial p/\partial z = -\rho g, \tag{2}$$

$$\partial \Theta/\partial t + \boldsymbol{u} \cdot \nabla \Theta + w \partial \Theta/\partial z = \partial (K_v \partial \Theta/z)/\partial z + \boldsymbol{F}_\Theta, \tag{3}$$

$$\nabla \cdot \boldsymbol{u} + \partial w/\partial z = 0, \tag{4}$$

$$\rho = \rho(T, S). \tag{5}$$

Here, $\boldsymbol{u}$ is the horizontal velocity with components (u, v), and w is the vertical component. ∇ is the horizontal nabla operator, $f = 2\Omega \sin(\phi)$ is the

Coriolis parameter, where $\Omega = 7.292 \times 10^{-5}$ s^{-1} and ϕ is the latitude, $\boldsymbol{k}$ is the vertical unit vector, ρ_0 is a reference density, p is pressure, g is the gravitational acceleration, z is the vertical coordinate (positive upwards), Θ represents either seawater temperature T or salinity S. The water density ρ is related to salinity and temperature through an equation of state (5) in accordance with UNESCO standards (UNESCO 1983). $\boldsymbol{F}_u$ and $\boldsymbol{F}_\Theta$ are Laplacian-type horizontal viscosity and diffusion terms, respectively, with coefficients A_H and K_H taken to be equal, modelled by Smagorinsky's (1963) formulation (for details see Oey & Chen 1992, AJ):

$$A_H = K_H = C\Delta\,\Delta y[u_x^2 + v_y^2 + 0.5(u_y + v_x)^2]^{1/2}, \tag{6}$$

where Δx and Δy are the horizontal grid distance and C is a numerical constant (assumed equal to 0.1 in our calculations).

The vertical eddy viscosity and diffusivities, A_v and K_v K_H, are calculated using the level-2.5 turbulence kinetic energy closure scheme of Mellor & Yamada (1982).

The boundary conditions are as follows.

At the sea surface ($z = \eta$):

$$A_v(\partial u/\partial z, \partial v/\partial z) = (\tau_x^s, \tau_y^s), \tag{7}$$

$$K_v(\partial T/\partial z, \partial S/\partial z) = (Q_{TS}, Q_{SS}), \tag{8}$$

with

$$Q_{TS} = \frac{Q_T}{\rho_0 c_{pw}} + Q_{TSR}, \tag{9}$$

$$Q_{SS} = \frac{Q_S}{\rho_0} + Q_{SSR}, \tag{10}$$

where (τ_x^s, τ_y^s) are components of the wind stress vector and Q_T, Q_S are heat and salinity fluxes.

The terms (Q_{TSR}, Q_{SSR}) in eqs. (9) and (10) express additional climatological heat and salinity fluxes used to drive the model in the case when real fluxes are very small, impossible to estimate from meteorological data, or absent altogether. This approach, called the method of 'relaxation towards climatology' is in common use in ocean models (cf. Oey & Chen 1992, Lehmann 1995, Svendsen et al. 1996). The additional surface heat and salinity fluxes Q_{TSR}, Q_{SSR} can be estimated as follows:

$$Q_{TSR} = C_{TC}(T_c - T); \qquad Q_{SSR} = C_{SC}(S_c - S), \tag{11}$$

where C_{TC}, C_{SC} – relaxation constants equal to $C_{TC} = 2$ m days^{-1} and $C_{SC} = 20$ m days^{-1}, respectively, T, S – calculated values of temperature and salinity in the surface layer, respectively, T_c, S_c – climatological values of temperature and salinity at the sea surface, respectively.

$$w = \partial\eta/\partial t + \boldsymbol{u}\nabla \cdot \eta. \tag{12}$$

At the sea bottom ($z = -H$):

$$A_v(\partial u/\partial z, \partial v/\partial z) = C_D \mid \boldsymbol{u}_b \mid \boldsymbol{u}_b, \tag{13}$$

$$K_v(\partial T/\partial z, \partial S/\partial z) = (0, 0), \tag{14}$$

$$w = -\boldsymbol{u} \cdot \nabla H. \tag{15}$$

Here, $\boldsymbol{u}_b$ is the horizontal velocity at the sea bottom, C_D is the drag coefficient equal to 0.0025.

At the lateral boundary $((x, y) \epsilon L)$:

$$U_n = \frac{c}{H} \eta; \quad c = (gH)^{1/2}. \tag{16}$$

$$(\boldsymbol{n} \cdot \boldsymbol{u})_t + C_i(\boldsymbol{n} \cdot \boldsymbol{u})_n = 0, \tag{17}$$

$$(T, S)_t + (\boldsymbol{n} \cdot \boldsymbol{u}_n)(T, S)_n = 0. \tag{18}$$

Here, $\boldsymbol{n}$ is a unit outward vector normal to the boundary line L, U_n is the depth – averaged velocity normal to the boundary, C_i is the internal phase speed taken to be a constant equal to $(gH \times 10^{-3})^{1/2}$.

Numerical solution

The numerical scheme used to solve the model equations is given in Blumberg & Mellor (1987) and in Mellor (1993). In brief, the momentum and mass transport equations, after having been transformed to the σ-coordinate system ($\sigma = \frac{z-\eta}{H+\eta}$, where η is the deviation of the free surface from its equilibrium position ($z = 0$) and H is the equilibrium depth of the water column), are solved numerically by finite-difference methods. The POM code uses the 'Arakawa C' numerical grid (cf. Mesinger & Arakawa 1976) and conserves both linear and quadratic quantities like mass, energy and vorticity. Time differencing is explicit in the horizontal and implicit in the vertical. Thus, time constraints due to the vertical grid are removed, permitting fine resolution in the surface and bottom boundary layers. The model has a free surface and can thus include atmospheric-induced sea level variations and free surface gravity waves. The time integration is therefore split into a two-dimensional (2-D), external mode with a short time step based on the Courant-Friedrichs-Lewy (CFL) (cf. Kowalik & Murthy 1993) stability conditions and calculated using the (fastest) free surface gravity wave speed, and a three-dimensional (3-D), internal mode with a long time step based on the CFL condition and calculated using the internal wave speed. Further details concerning the numerical schemas used in the POM code can be found in Mellor (1993).

In our calculations horizontal space steps of $\Delta\lambda = 5.4'$ and $\Delta\phi = 2.7'$ (i.e. a grid size of $\Delta x \simeq \Delta y \simeq 5$ km) were used. In the vertical, 24 σ-levels were applied with the distribution: 0.0, –0.00329, –0.00658, –0.01316, –0.02632, –0.05263, –0.10526, –0.15789, –0.21053, –0.26316, –0.31579,

–0.36842, –0.42105, –0.47368, –0.52632, –0.57895, –0.63158, –0.68421
–0.73684, –0.78947, –0.84211, –0.89474, –0.94737, –1.0. The time steps for
the external 2-D and internal 3-D calculations were 10 sec and 10 min,
respectively.

3. Initial conditions and atmospheric forcings

The same methodology was applied as described in detail in AJ. The
calculation was initiated with the climatological data for September. The
initial distribution of salinity and temperature was derived from the monthly
climatological data set of Lenz (1971) and Bock (1971).

The model was forced by winds, air pressure and surface heat fluxes
estimated on the basis of meteorological data taken from BED (2000).

3.1. Initial fields and climatological forcing

The initial 3-D fields of the seawater temperature T and its salinity
S in September were constructed from the monthly mean (multi-year
averaged) maps taken from Bock's (1971) and Lenz's (1971) atlases and
additional *in situ* data from The Regional Oceanographic Database of
IO PAS (http://www.iopan.gda.pl) recorded in September for several years.

The climatological forcings for September were calculated in the follow-
ing way. The two-dimensional fields of the temperature T and salinity S
at the sea surface for August, September and October were taken from the
monthly mean (multi-year averaged, climatic) surface maps in Bock's (1971)
and Lenz's (1971) atlases. Next, the 2-D fields of T and S were linearly
interpolated in time with an interval equal to the internal time step.

3.2. Atmospheric forcing

In order to estimate the wind stress components (τ_x^s, τ_y^s) and the heat
flux at the sea surface (Q_T), the standard way of utilizing the bulk formulas
commonly used in modelling, was applied (cf. e.g. Oey & Chen 1992,
Lehmann 1995, Meier et al. 1999).

Wind stress

The wind stress components at the sea surface (τ_x^s, τ_y^s) (eq. (7)) are
calculated using standard formulas (cf. Lehmann 1995, AJ):

$$\tau_x = \rho_a c_D W_x W_a; \quad \tau_y = \rho_a c_D W_y W_a, \tag{19}$$

with the drag coefficient c_D according to Large & Pond (1981):

$$c_D 10^3 = \begin{cases} 1.14 & \text{if} \quad W_a \leq 10\,\text{m}\,\text{s}^{-1} \\ (0.49 + 0.065 W_a) & \text{if} \quad 10\,\text{m}\,\text{s}^{-1} \leq W_a \leq 25\,\text{m}\,\text{s}^{-1}, \end{cases} \tag{20}$$

where W_a, W_x, W_y – absolute value (modulus) and components, respectively, of the 'real' wind vector at standard height above the free sea surface, ρ_a – air density.

The 'real' wind speed W_a was estimated from the quasi-geostrophic wind model (see AJ for details) with the reduction coefficient of the geostrophic wind speed (W_{ag}) due to friction in the marine atmospheric boundary layer $C_r = 0.7$ and together with an ageostrophic angle equal to $\alpha_{ag} = 15°$.

Heat flux at the sea surface

The total heat flux through the sea surface Q_T in eq. (9) is estimated from a simplified version of the heat budget of the sea surface:

$$Q_T = R_a - Q_B + Q_H + Q_E, \tag{21}$$

where
Q_T – the total net heat flux across the sea surface,
R_a – incoming solar radiation at the sea surface,
Q_B – the longwave radiation flux of the sea surface,
Q_H – the sensible heat flux,
Q_E – the latent heat flux.

The net flux of longwave radiation of the sea surface is calculated by the formula (Stevenson 1982):

$$Q_B = [\epsilon\sigma_S T_w^4(0.39 - 0.05e_{10}^{1/2}) + 4\epsilon\sigma_S T_w^3(T_w - T_{10})]g_{cs}(N), \tag{22}$$

where
$\epsilon = 0.97$ is the sea surface emissivity,
σ_S – the Stefan-Boltzmann constant (equal to 5.673×10^{-8} W m^{-2} K^{-4}),
$e_{10} = p_a/(1 + 0.62197/q_{10})$ – the water vapour pressure (in mb) at a height of 10 m above the free sea surface,
T_w – the sea surface temperature in °K,
T_{10} – the air temperature in °K at a height of 10 m above the free sea surface, $g_{cs}(N)$ the relationship describing the reduction of the longwave radiation due to the cloudiness ratio N,
p_a – the atmospheric pressure at the sea surface,
W_a – the modulus of wind speed at the standard height above the free sea surface.

The net sensible heat flux Q_E and the net latent heat flux Q_E are calculated by the standard bulk formulas:

$$Q_H = \rho_a c_{pa} C_{H10} W_a(t_w - t_{10}); \tag{23}$$

$$Q_E = \rho_a C_{E10} L_E W_a(q_s - q_{10}), \tag{24}$$

where
c_{pa} – the specific heat capacity of air ($c_{pa} = 1.008 \times 10^3$ J kg^{-1} K^{-1}),

W_a – the modulus of wind speed at the standard height above the sea surface,

C_{H10}, C_{E10} – the transfer coefficients for heat and humidity, respectively,

t_w, t_{10} – the seawater temperature and air temperature at standard height,

L_E – the specific latent heat of evaporation (~ 2.5 x 10^6 J kg^{-1}),

q_{10} – the specific humidity at standard height above the sea surface,

q_s – the specific humidity of the atmosphere close to the sea surface.

The transfer coefficients C_{H10} and C_{E10} are parameterized by the method of Launiainen (1979) (see also Jankowski & Masłowski 1991). For details of the estimation of the radiation R_a, the reader is referred to AJ.

4. Results

4.1. Methodology and strategies of computations

The model simulations were performed in two stages. In both stages the river runoff rates (assumed as yearly means) of the 31 main rivers in the Baltic Sea catchment area were taken into consideration.

The first stage, a 20-day pre-processing run, was used to initialize the model computations. At this stage the model started from the three-dimensional initial distribution of temperature and salinity and was forced only by the climatological forcings, without external atmospheric forcing or heat fluxes. The initial fields of sea level η, the current velocity vector components u, v, w, and the mean-depth current components U, V were set equal to 0.

The climatological forcings were coupled to the model by means of the so-called method of 'relaxation towards climatology' (cf. Oey & Chen 1992, Lehmann 1995, AJ), i.e. the transport equations for heat and salt (eq. (3)) were solved with the surface boundary condition (eq. (8)) reduced to the form

$$K_v(\partial T/\partial z, \partial S/\partial z) = (Q_{TSR}, Q_{SSR}), \tag{25}$$

with Q_{TSR} and Q_{SSR} estimated according to eq. (11).

An adaptation of the model dynamics to the initial fields and climatology was achieved by a forward integration of the model equations over a period of 20 days after which a quasi-stationary state was reached.

The second stage was started from the previous stage's final results. and consisted of a fully prognostic run. Besides climatological forcings, the model was now forced by real atmospheric forcings (atmospheric pressure, winds and heat fluxes) for a period of 30 days (1 to 30 September 1989). At this stage the transport equations for heat and salt (eq. (3)) were solved

with the surface boundary condition (eq. (8)) in full form. In the simulations presented here, the salinity flux Q_S at the sea surface was assumed to be negligible and was set equal to 0.

4.2. Model results and discussion

The meteorological data for calculating real atmospheric forcings (atmospheric data: pressure, air temperature, relative humidity) was taken from BED (2000) for the entire simulation period (from 1–30 September 1989). The meteorological data provided every 3 h on a $1° \times 1°$ grid were mapped on to a numerical model grid and linearly interpolated to the model grid.

The hindcast calculations were performed along with the methodology and strategies decribed in the previous sections.

Although model runs were performed for the entire Baltic Sea, this presentation of the hindcast simulation results is limited to the coastal area along the Polish Baltic coast ($13°30'E$–$20°06'E$; $53°30'N$–$55°30'N$) (cf. Fig. 3), where an upwelling-like large fall in sea suface temperature at two coastal stations was observed (Malicki & Miętus 1994).

Wind conditions

With reference to the overall atmospheric situation (Fig. 2) some details of wind forcing in September 1989 in the vicinity of the two coastal stations at Kołobrzeg and Władysławowo are given. Figs. 4 and 5 present time series of wind speed and its direction during model simulations at point K (off Kołobrzeg, sea depth 12 m) and W (off Władysławowo, sea depth 15 m). The location of these points on the Polish coast is shown in Fig. 3.

From these figures it follows that the wind forcing over the coastal area in September 1989 can be roughly characterized by a number of phases. Winds from NW and W were dominant during the first phase (1 to 7 September), with short interruptions on 1 and 4 September. On 8 September the wind veered E backing NE, and continued to blow from that sector for the rest of the second phase, until 12 September. On that day the winds backed rapidly to NW (W), after which the direction fluctuated from S to W for a period of 1–2 days, which was then followed by winds from SE (from 21 to 23 September). On 24 September the wind rapidly changed direction to N, NW and SW until the end of month, with an interruption to NE on 27 September. The wind speed (Fig. 5) fluctuated with a period of 2–3 days and an amplitude ranging from 3 to 7 m s^{-1}.

Time series of temperature and salinity at two selected points

Figs. 6 and 7 depict the temporal history of the calculated seawater temperatures in the surface layer at selected depths at points K and W.
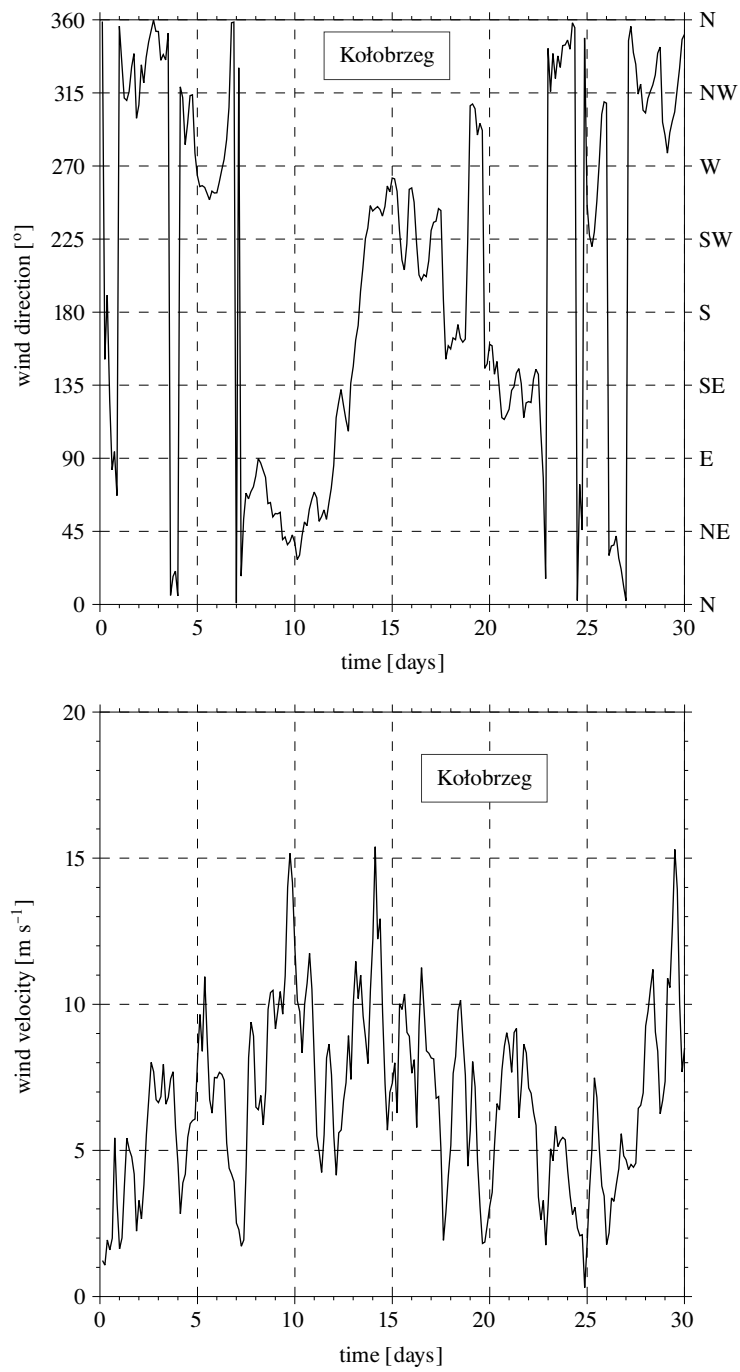
Fig. 4. Temporal evolution of velocity [m s^{-1}] and wind direction [°] at point K (off Kołobrzeg) in September 1989. Location of point – see Fig. 3
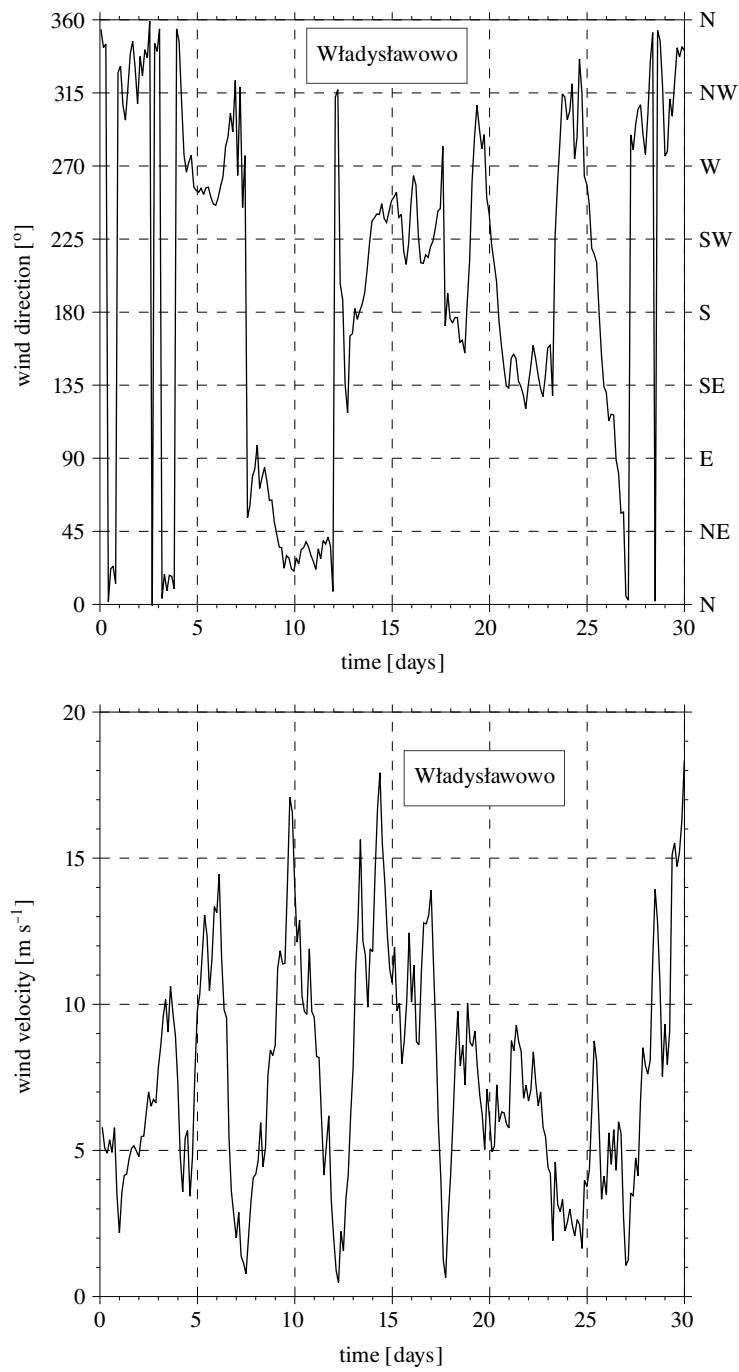
Fig. 5. Temporal evolution of velocity [m s^{-1}] and wind direction [°] at point W in the vicinity of Władysławowo in September 1989. Location of point – see Fig. 3
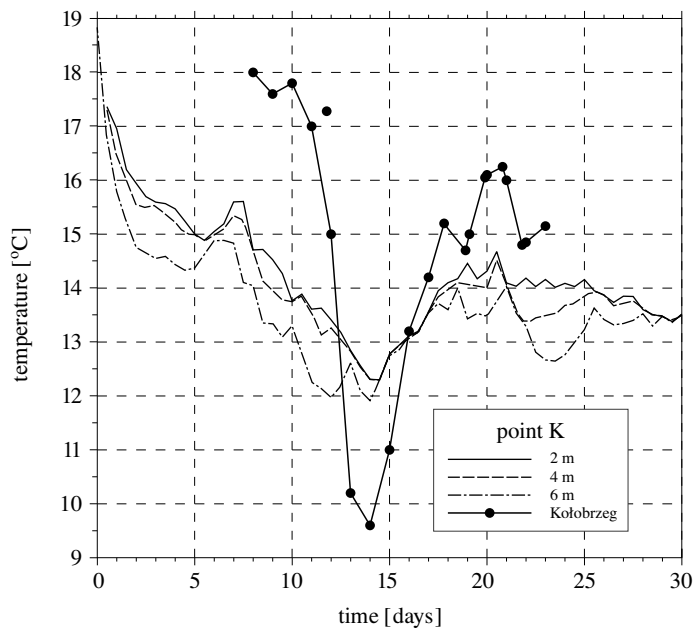
Fig. 6. Temporal evolution of the calculated seawater temperature [°C] at selected depths at point K (in the vicinity of Kołobrzeg). The sea surface layer temperatures at the Kołobrzeg station taken from Malicki & Miętus (1994) are also depicted (cf. Fig. 1). Location of point – see Fig. 3

For comparison with *in situ* observations the time series of seawater temperature taken from the figure in Malicki & Miętus (1994) were added Figs. 6 and 7.

From these figures it can be seen that the model gave a good reproduction of the fluctuations in time of the seawater temperature in the surface layer at both K and W, but the model results are underestimated by an average of 2–3°C. The simulated upwelling-like fall of temperature was not as large as the observed one. This is probably due to the methodology of computations (for details see Section 4.1). For short-term modelling, initialization of the model is essential. In order to improve the modelling results beyond what is at present possible, good quality fine-gridded *in situ* data have to be available.

The model and observed data were well synchronized to the timing and duration of variations of speed and especially, to changes in wind direction.

To complete the details of the variability in hydrological parameters, the time series of the calculated sea water salinity at selected depths at both points are presented in Figs. 8 and 9. Time series of the calculated salinity correlate well with the fluctuations in wind direction and the temporal
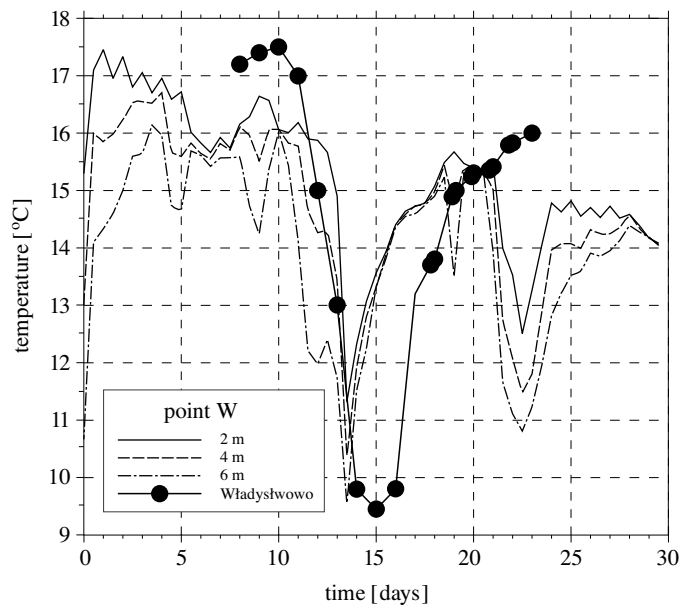
Fig. 7. Temporal evolution of the calculated seawater temperature [°C] at selected depths at point W (in the vicinity of Władysławowo). The sea surface layer temperatures at the Władysławowo station taken from Malicki & Miętus (1994) are also depicted (cf. Fig. 1). Location of point – see Fig. 3
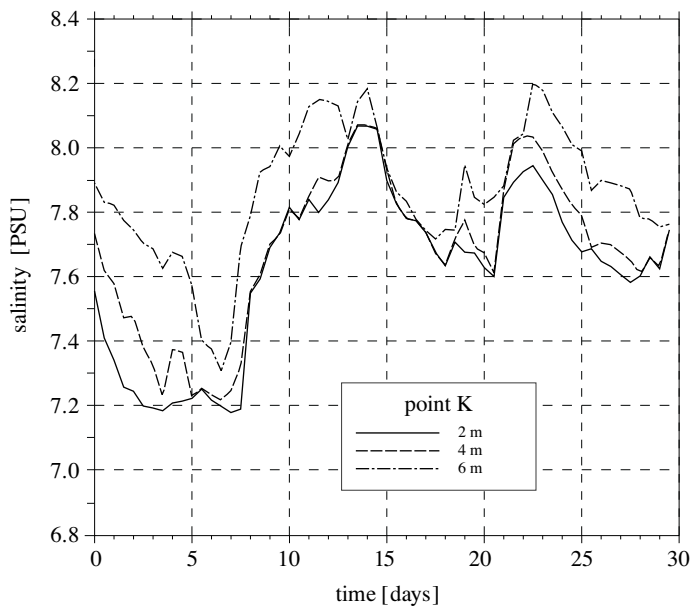

Fig. 8. Temporal evolution of the calculated seawater salinity [PSU] at selected depths at point K (in the vicinity of Kołobrzeg). Location of point – see Fig. 3
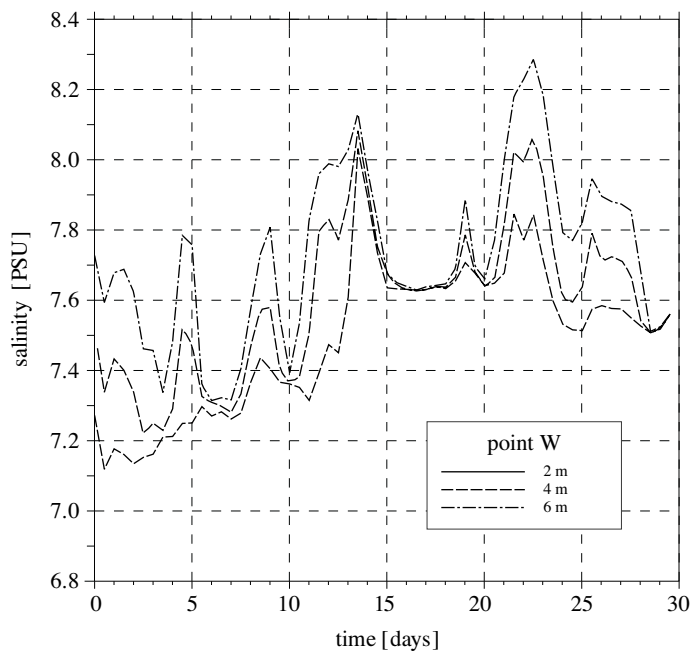
Fig. 9. Temporal evolution of the calculated sea water salinity [PSU] at selected depths at point W (in the vicinity of Władysławowo). Location of point – see Fig. 3

variability of temperature in the surface layer at both sites. The maxima of the observed large fall in the surface temperatures and of the rise in salinity in the surface layers at both points are closely correlated with the phase of the change of the upwelling-favourable wind direction (E, NE) to the opposite one (see Figs. 4 and 5 for the temporal history of the wind direction).

Temperature distribution and current patterns

The output data of the numerical simulations were stored every 12 hours at selected depths in order to analyse the spatial and temporal variability of the fields of hydrophysical parameters during the modelled upwelling-like event in September.

Figs. 10 a–h present a series of snapshots of seawater temperature at 2 m depth and the current patterns at 10 m depth in a time sequence of 1 day from 10 to 17 September.

They demonstrate the temporal history of the occurrence of coastal upwelling, its 2–3 day evolution and its disappearence in the southern Baltic along the Polish coast in September 1989. The simulated circulation patterns complete the spatial picture of hydrodynamic conditions related to
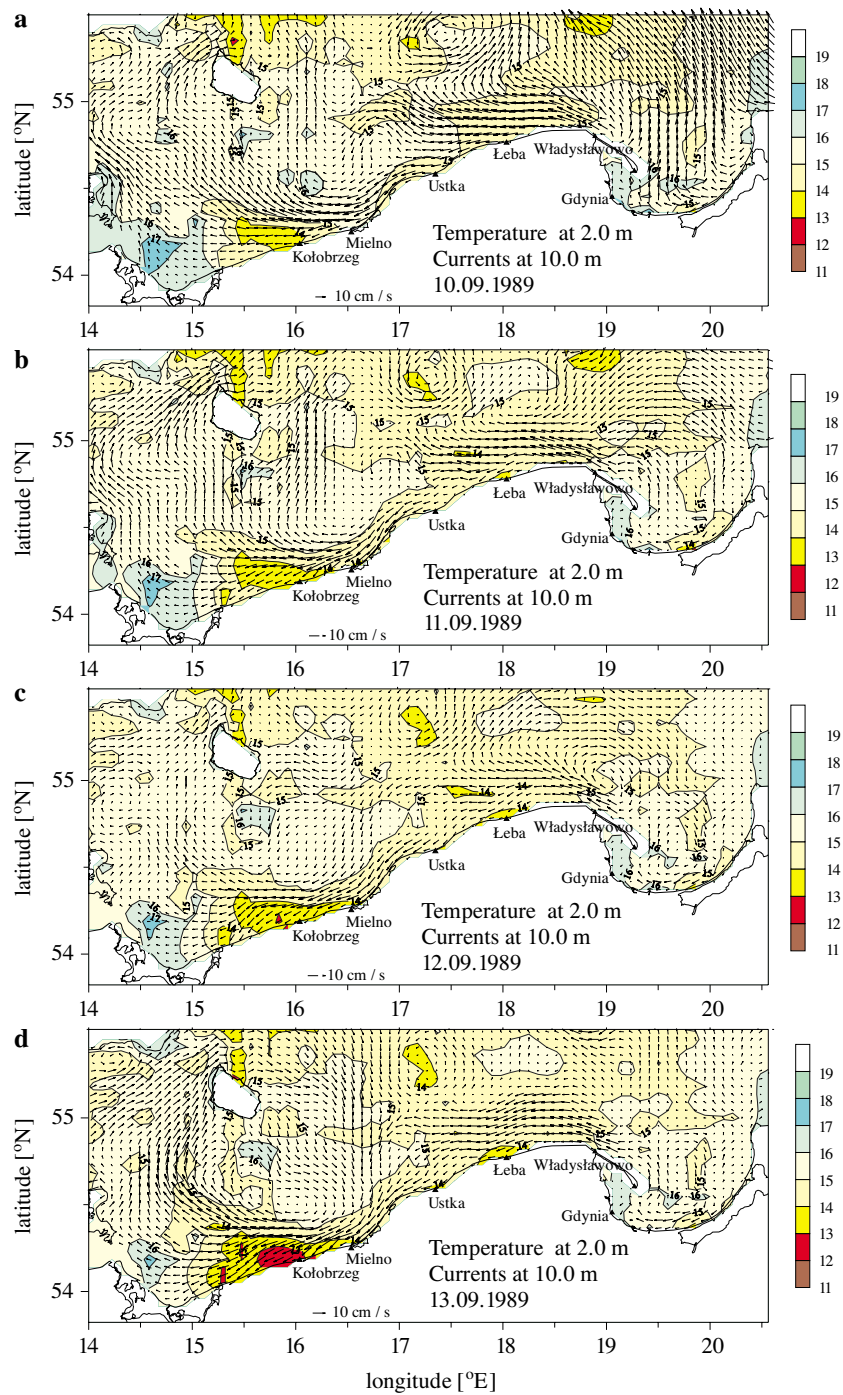
Fig. 10. Simulated seawater temperature [°C] in the surface layer and current vectors at 10 m depth in a time sequence of 1 day from 10.09.1989 to 17.09.1989 (a–h)
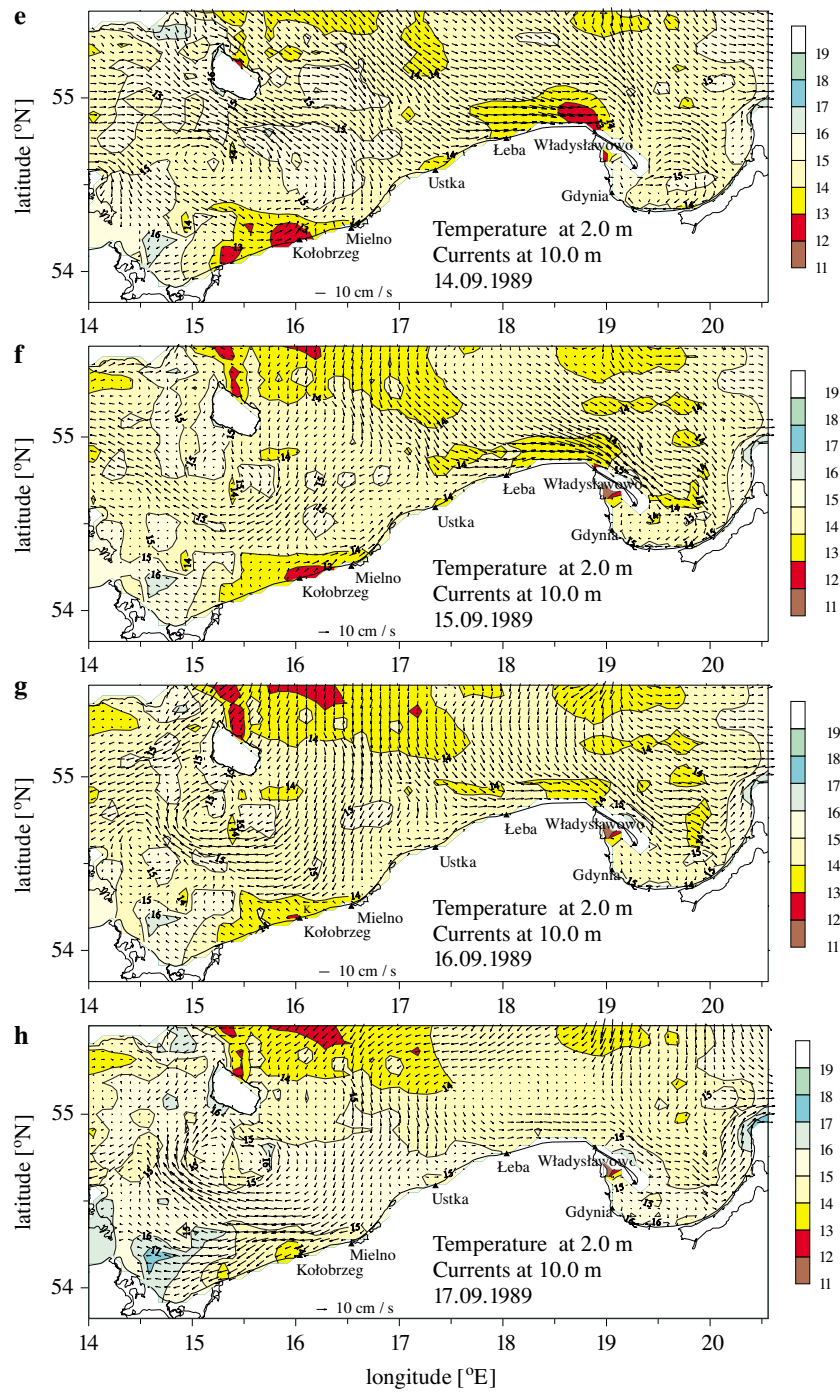
Fig. 10. (*continued*)

the upwelling-like event. Current vectors at 10 m depth illustrate the overall picture and the variability of water exchange between the coastal zone and the open sea related to the variability of forcing. It is a straightforward matter to discover from the above figures that the evolution of the dynamic situation is closely related to the variability of atmospheric forcing (wind direction).

Analysis of the above figures confirms that not only the subtleties of the bottom topography but also the shoreline configuration relative to the wind direction contribute to the variability in seawater temperature and circulation patterns.

The results of hindcast simulations show that under real atmospheric forcing in September 1989, near the Polish Baltic coast an intensive time-variable upwelling-like process developed, as a result of which the hydrological conditions in the coastal area were substantially modified.

Characteristic features of the coastal water dynamics can be followed from the model results: (i) a coastal jet along the open-sea coast during the upwelling-favourable wind phase; (ii) the transient character of water movements highly variable in time and space; (iii) two, fairly readily distinguishable regimes of water dynamics and water exchange between the open sea and the coastal zone along the Polish coast – to the east and west of the Słupsk Bank; (iv) the peculiar hydrodynamic conditions along the Hel Peninsula.

A comparison of the spatial temperature distributions and current patterns (Figs. 10 a–h) with the bottom topography of the southern Baltic Sea (Fig. 3) shows that the bottom topography variations and coastline configuration play an important role in the development of the mesoscale features of the coastal hydrodynamics in this area. The Słupsk Bank controls the dynamics of the open-sea coastal waters and, in consequence, two different dynamic regimes can be observed: to the east and to the west of it. In the western part the water movements are closely correlated with the dynamics of offshore waters (the Bornholm Basin) whereas those in the eastern part are under the influence of the eastern Gotland Basin, the Gdańsk Deep and the Słupsk Furrow, all regions with a complex bottom topography (see Fig. 5 for details). Here, because of the Hel Peninsula and the topographical variations in its vicinity, special hydrodynamic conditions arise in response to wind forcing. This supports the findings from Krężel's work (1997), which was based on an analysis of satellite images, that specific conditions are required for upwelling to occur off the Hel Peninsula. But it is necessary to mention that in this paper as in Nature, we are dealing with a time-variable upwelling. It generates hydrological conditions that are to some extent different from steady upwelling. The latter model is usually used

to interpret or understand the results of *in situ* observations. This approach may be applied correctly only to hydrological events due to special steady or long-term averaged forcing conditions.

5. Conclusions

The 3-D circulation baroclinic model of the Baltic Sea, based on the Princeton Ocean Model code of Mellor (1993), was applied to a hindcast numerical simulation of an upwelling-like event – a rapid fall in surface seawater temperature, observed in the coastal area of the southern Baltic in September 1989.

The model provided a good reproduction of the temporal history of seawater temperature in the surface layer reported from two sites on the Polish Baltic coast: in the vicinity of Kołobrzeg and Władysławowo, but the model results are underestimated.

The maximum drop in the surface layer temperature and rise in salinity in the surface layers at those two sites are closely correlated to the phase of change of the upwelling-favourable wind direction.

The current patterns and the variability in temperature distributions during the main phase of time-varying upwelling are presented. The variability of the modelled hydrophysical parameters confirm the occurrence of an upwelling-like situation between 8 and 17 September. The model results showed up the important role of the variability of the wind field and the topography of the bottom as well as the coastline in the evolution of the spatial structure of thermohaline and current velocity fields.

The model simulations enabled some characteristic features of the coastal water dynamics on the Polish coasts in September 1989 to be discovered. The bottom features of the Słupsk Bank seem to be decisive in governing the hydrodynamics, and two hydrological regimes, one in the eastern part of coast and a second in the western one, can be observed. In the western part, along the Hel Peninsula, specific conditions for the occurrence and development of upwelling-like processes were found.

Although the paper gives only a description and a preliminary discussion of the simulated coastal water hydrodynamics in September 1989, it may be useful for a better understanding of the mesoscale features of the water dynamics induced by real atmospheric forcing along the Polish Baltic coast.

References

BED, 2000, *Atmospheric inputs*, [in:] *The BED database*, http://data.ecology.su.se/Models/bedcontent.htm.

Blumberg A. F., Mellor G. L., 1987, *A description of a three-dimensional coastal ocean circulation model*, pp. 1–16, [in:] *Three-dimensional coastal ocean models*, N. S. Heaps (ed.), Am. Geophys. Union, 4, 208 pp.

Bock K.-H., 1971, *Monatskarten des Salzgehaltes der Ostsee, dargestellt für verschiedene Tiefenhorizonte*, Dt. Hydrogr. Z., 12, 148 pp.

Bychkova I. A., Viktorov S. V., 1987, *Elucidation and systematization of upwelling zones in the Baltic Sea based on satellite data*, Okieanologiya, 27, 218–223, (in Russian).

Bychkova I. A., Viktorov S. V., Shumakher D. A., 1988, *A relationship between the large-scale atmospheric circulation and the origin of coastal upwelling in the Baltic Sea*, Meteor. Gidrol., 10, 91–98, (in Russian).

Csanady G. T., 1982, *Circulation in the Coastal Ocean*, D. Reidel Publ. Co., Boston, MA, 279 pp.

Fennel W., Seifert T., 1995, *Kelvin wave controlled upwelling in the western Baltic*, J. Mar. Sys., 6, 286–300.

Fennel W., Sturm M., 1992, *Dynamics of the western Baltic*, J. Mar. Sys., 3, 183–205.

Gidhagen L., 1984, *Coastal upwelling in the Baltic Sea*, Proc. 14th Conf. Baltic Oceanographers, Gdynia, vol. 1, 182–190.

Gill A. E., 1982, *Atmoshere-Ocean Dynamics*, Acad. Press, New York, 662 pp.

Gill A. E., Clarke A. J., 1974, *Wind-induced upwelling, coastal currents and sea-level changes*, Deep-Sea Res., 21, 325–345.

Haapala J., 1994, *Upwelling and its influence on nutrient concentration in the coastal Area of the Hanko Peninsula, Entrance of the Gulf of Finland*, Estuar., Coast. Shelf Sci., 38, 507–521.

Hansen L., Højerslev N. K., Soogaard H., 1993, *Temperature monitoring of the Danish marine environment and the Baltic Sea*, Københavns Univ., Rep. No. 52, 77 pp.

Jankowski A., 2000, *Wind induced variability of hydrological parameters in the coastal zone of the southern Baltic Sea – numerical study*, Oceanol. Stud., 29 (3), 5–34.

Jankowski A., 2002, *Application of a σ-coordinate baroclinic model to the Baltic Sea*, Oceanologia, 44 (1), 59–80.

Jankowski A., Masłowski W., 1991, *Methodological aspects of wind momentum, heat and moisture fluxes evaluation from the standard hydrometeorological measurements on board a ship*, Stud. i Mater. Oceanol., 58, 63–76.

Kowalewski M., 1998, *Coastal upwellings in a shallow stratified sea, for example, in the Baltic Sea*, Ph. D thesis, Uniw. Gd., Gdynia, 85 pp., (in Polish).

Kowalik Z., Murty T. S., 1993, *Numerical modeling of ocean dynamics*, Adv. Ser. on Ocean Eng., 5, World Sci., Singapore–New Jersey–London–Hong Kong, 481 pp.

Krężel A., 1997, *Recognition of mesoscale hydrophysical anomalies in a shallow sea using broadband satelitte teledetection methods*, Wyd. Uniw. Gd., Gdańsk, 173 pp., (in Polish).

Large W. G., Pond S., 1981, *Open ocean momentum flux measurements in moderate to strong winds*, J. Phys. Oceanogr., 11, 324–336.

Launiainen J., 1979, *Studies of energy exchange between the air and the sea surface on the coastal area of the Gulf of Finland*, Finnish Mar. Res., 246, 3–110.

Lehmann A., 1995, *A three-dimensional baroclinic eddy-resolving model of the Baltic Sea*, Tellus, 47 (A), 1013–1031.

Lenz W., 1971, *Monatskarten der Temperatur der Ostsee, dargestellt für verschiedene Tiefenhorizonte*, Dt. Hydrogr. Z., 11, 148 pp.

Malicki J., Miętus M., 1994, *Climate*, pp. 60–69, [in:] *The Baltic Sea atlas*, A. Majewski & Z. Lauer (eds.), Inst. Meteor. i Gosp. Wod., Warszawa, 214 pp., (in Polish).

Matciak M., Urbański J., Piekarek-Jankowska H., Szymelfenig M., 2001, *Presumable groundwater seepage influence on the upwelling events along the Hel Peninsula*, Oceanol. Stud., 30 (3)–(4), 125–132.

Meier H. E. M, 1999, *First results of multi-year simulations using a 3D Baltic Sea model*, SMHI, Rep. Oceanogr. No. 27, 1–48.

Meier H. E. M, Döscher R., Coward A. C., Nycander J., Döös K., 1999, *RCO – Rossby Centre regional Ocean climate model: model description (version 1.0) and first results from the hindcast period 1992/93*, SMHI, Rep. Oceanogr. No. 26, 1–102.

Mellor G. L., 1993, *User's guide for a three-dimensional, primitive equation, numerical ocean model*, Prog. Atmos. Ocean. Sci., Princeton University, 35 pp.

Mellor G. L., Yamada T., 1974, *A hierarchy of turbulence closure models for planetary boundary layers*, J. Atmos. Sci., 13, 1791–1806.

Mellor G. L., Yamada T., 1982, *Development of a turbulent closure model for geophysical fluid problems*, Rev. Geophys., 20, 851–875.

Mesinger F., Arakawa A., 1976, *Numerical models used in atmospheric models*, GARP Publ. Ser., 17 (1), WMO–ICSU, 64 pp.

Oey L.-Y., Chen P., 1992, *A model simulation of circulation in the northeast Atlantic shelves and seas*, J. Geophys. Res., 97, 20087–20115.

Robinson I. S., 1985, *Satellite oceanography: an introduction for oceanographers and remote-sensing scientists*, Ellis Horwood Limited, Chichester, 455 pp.

Schmidt M., Seifert T., Lass H.-U., Fennel W., 1998, *Patterns of salts propagation in the Southwestern Baltic Sea*, Dt. Hydrogr. Z., 50, 345–364.

Seifert T., Kayser B., 1995, *A high resolution spherical grid topography of the Baltic Sea*, Meereswissensch. Ber., Inst. für Ostseeforschung, Warnemünde, 9, 72–88.

Siegel H., Gerth M., Rudloff R., Tschersich G., 1994, *Dynamic features in the western Baltic Sea investigated using NOAA–AVHRR Data*, Dt. Hydrogr. Z., 46, 191–209.

Smagorinsky J., 1963, *General circulation experiments with the primitive equations. I. The basic experiment*, Mont. Weather Rev., 91, 99–164.

Smith R. L., 1968, *Upwelling*, Oceanogr. Mar. Biol., Ann. Rev., 6, 11–46.

Stevenson J. W., 1982, *Computation of heat and momentum fluxes at the sea surface during the Hawaii to Tahiti Shuttle Experiment*, Joint Inst. Mar. Atmos. Res. Univ. of Hawaii No. 82–0044, Honolulu, 42 pp.

Svansson A., 1975, *Interaction between the coastal zone and the open sea*, Finnish Mar. Res., 239, 11–28.

Svendsen E., Berntsen J., Skogen M., Ådlandsvik B., Martinsen E., 1996, *Model simulation of the Skagerrak circulation and hydrography during Skagex*, J. Mar. Sys., 8, 219–236.

UNESCO, 1983, *Algorithms for the computation of fundamental properties of sea water*, UNESCO Tech. Pap. Mar. Sci., 44, 53 pp.

Urbański J., 1995, *Upwellings along the Polish coasts of the Baltic Sea*, Prz. Geofiz., 40, 141–153, (in Polish).